JCTC Journal of Chemical Theory and Computation

Characterization of Chitin and Chitosan Molecular Structure in Aqueous Solution

Eduardo F. Franca,[†,‡] Roberto D. Lins,*[,†] Luiz C. G. Freitas,[‡] and T. P. Straatsma[†]

Pacific Northwest National Laboratory, Richland, Washington 99352, and Departamento de Química, Universidade Federal de São Carlos, São Carlos, SP, Brazil

Received July 24, 2008

Abstract: Molecular dynamics simulations have been used to characterize the structure of single chitin and chitosan chains in aqueous solutions. Chitin chains, whether isolated or in the form of a β-chitin nanoparticle, adopt the 2-fold helix with ϕ and φ values similar to its crystalline state. In solution, the intramolecular hydrogen bond $HO3_{(n)}\cdots O5_{(n+1)}$ responsible for the 2-fold helical motif in these polysaccharides is stabilized by hydrogen bonds with water molecules in a well-defined orientation. On the other hand, chitosan can adopt five distinct helical motifs, and its conformational equilibrium is highly dependent on pH. The hydrogen bond pattern and solvation around the O3 atom of insoluble chitosan (basic pH) are nearly identical to these quantities in chitin. Our findings suggest that the solubility and conformation of these polysaccharides are related to the stability of the intrachain $HO3_{(n)}\cdots O5_{(n+1)}$ hydrogen bond, which is affected by the water exchange around the O3-HO3 hydroxyl group.

Introduction

Chitin is the second most abundant organic material in nature after cellulose. It is a naturally occurring glucose-derivative polymer forming the primary component of fungal cell walls, arthropods, and certain algaes. Chitosan, its main derivative, is the partly N-deacetylated chitin. Deacetylation level almost never reaches 100%. It is generally accepted that this biopolymer is considered as chitosan if chitin is N-deacetylated to such a degree that it becomes soluble in dilute acidic medium, which is typically on the order of 40−60%.[1] The amine groups of the chitosan glucosamine units ($pK_a \sim 6.3-6.5$) are important chelation sites for metal ions in neutral to alkaline conditions and form stable complexes with anions by electrostatic interactions in acidic conditions.[2−5] Unlike chitin, chitosan is positively charged in acidic to neutral conditions with a net charge density, and therefore its adsorption capacity is dependent on pH and N-deacetylation level.[6−8] The overall metal- and anion-binding capacities of these polymers result from the interplay between the degree of deacetylation, molecular weight, surface area, and crystallinity. Because of chitin and chitosan widespread availability, and of their strong affinity for ions, molecules, macromolecules and even microorganisms, a great variety of chitosan particles is engineered for an impressively wide range of applications including the following: removal of toxic radionuclide and heavy metals, recovery of precious metals, nitrogen fertilization in agriculture, pesticide removal, fine clay particle stabilization/coagulation (e.g. on some U.S. Department of Transport highways), alkaline fuel cell, tissue-engineering (e.g., fibers, textiles), biomaterial stabilization, catalysis support, food emulsification, paper food, fungal and bacterial disease prevention, drug delivery, pharmaceutical excipients, and as blood plasma cholesterol and intestinal triglycerides regulation in the human body.[9−15]

Natural chitin has three anhydrous crystalline polymorphs, α-, β-, γ-chitins, in the native state, which is found in the skeletal structure of crustaceans, insects, mushrooms, and the cell wall of fungi.[16] The structure of α and β forms differ only in that the piles of chains are arranged alternately antiparalel in a α-chitin, whereas they are all parallel in β-chitin.[17] The γ-chitin form has characteristics of both α and β forms, where two chains run in one direction and another chain in the opposite direction; however, it is considered only a variant of the α family, because it has the same properties as the α-chitin.[18] α-Chitin is the most abundant and also the

* Corresponding author phone: (509)375-2755; fax: (509)372-4720; e-mail: roberto.lins@pnl.gov.

[†] Pacific Northwest National Laboratory.

[‡] Universidade Federal de São Carlos.

10.1021/ct8002964 CCC: $40.75
Published on Web 11/08/2008

most stable thermodynamically,[19,20] and the β- and γ-chitin forms can be irreversibly converted into the α-form.[16] Chitosan has anhydrous and hydrated forms, with piles chains arranged in an antiparallel fashion.[21−23]

Experimental results obtained using various methods of polymer structure investigations (IR spectroscopy, NMR, X-ray scattering, microscopy, sorption techniques) showed that chitin and chitosan, just as cellulose, are characterized by an ordered fibrillar structure, a developed system of intra- and intermolecular hydrogen bonds, a high degree of crystallinity, and polymorphism.[13,24] According to X-ray crystallography experiments, chitin is a linear polysaccharide where the chains composed of 2-acetamido-2-deoxy-D-glucopyranose and linked by β-(1→4) glycoside bonds on a 2_1 screw axis have a repeating unit of 1.030 to 1.043 nm.[25−27] Similarly to chitin, both hydrated and the anhydrous forms of chitosan have a conventional extended 2-fold helical conformation with a repeating pattern every ca. 1.0 nm,[21,28] although acid salts of chitosan can favor different structural arrangements.[23] Three types of structural complexes have been observed for chitosan and can be classified according to their chain repeating unit. The first type, so-called type I form, is the anhydrous form, where in these crystals the backbone chitosan chains retain the extended 2-fold helix of the unreacted chitosan molecule.[21] The type II is a hydrated crystal with a chain repeat about 4.08 nm and asymmetric unit (repeating units) consisting of four glucosamine residues. Since two tetrasaccharides make a chain repeat, this is also a 2-fold helix even though the conformation is completely different to that of type I form, where the asymmetric unit is one glucosamine residue. Type II form is also known as relaxed 2-fold helix because it is almost four times longer than unreacted chitosan.[29,30] A type II salt variant, called type IIa, has a similar chain repeat (4.05 nm), but the molecular conformation is a 4/1 helix, with an asymmetric unit consisting of a glucosamine dimer. This right-handed helix comprises four asymmetric units.[30] The most recently discovered form, type III, has a chain pattern with a chain repeat of 2.55 nm, a 5-fold helix, and an asymmetric unit of one glucosamine residue.[31]

It is well-known that hydrogen bonds play an important part in the stabilization of secondary structures of proteins. Likewise, it has been proposed that the structure of chitin and chitosan chains are also stabilized by two hydrogen bonds, one intrachain and one interchain.[32] An intramolecular hydrogen bond is formed between atoms HO3 and O5 of consecutive linked glucosamine units. This intramolecular hydrogen bond ($HO3_{(n)}\cdots O5_{(n+1)}$) is responsible for the length of the chain repeating distance and to keep the chitin chain in a 2-fold helical pattern.[25,33] There are two possibilities of intermolecular hydrogen bonds in the solid state, between two N-acetyl groups (e.g., $N-H_{(i)}\cdots O{=}C_{(j)}$) and between one N-acetyl and a hydroxymethyl group. In α-chitin, each amounts for roughly 50% of the interchain interactions.[13] The latter pattern has not been reported in the crystal structures of β-chitin and is thought to account for the increased susceptibility to crystalline swelling of β-chitin.[13] The hydrogen bond network is responsible for linking the chitin chains in arranged bonded piles or sheets.[19,26]

Other studies using X-ray crystallography,[27] ^{13}C solid-state NMR,[20] and molecular dynamics simulations[34] showed further information about the hydrogen bonds and conformations of the hydroxymethyl and the N-acetyl groups in solid state. However, there are no studies that described the dynamical properties of these hydrogen bonds and the possible orientations of these groups in chitin upon solvation. The only molecular study involving the presence of water as solvent is the X-ray structure of the monohydrate form of the chitin $[C_8H_{13}O_5N(H_2O)]_n$.[35] This study showed that water molecules taking part in the hydrogen bond system of chitin are stable and not unusual. Hydroxyl groups were found to be the main partners in the hydrogen bonds involving water molecules, which have a typical distance of 2.8 Å. (A hydrogen bond is assumed to be present when the hydrogen-acceptor distance is less than 3.5 Å and the donor-hydrogen-acceptor angle is larger than 135°.) Like chitin, the structure of chitosan also displays hydrogen bonds between the $O3_{(n)}$ and $O5_{(n+1)}$ oxygen atoms across the glycosidic linkages and by interchain hydrogen bonds involving the oxygen atom of the hydroxymethyl group (O6) of one chain and the amine nitrogen atom (N2) of the D-glucosamine unit of another chain. The patterns in polymer packing are therefore highly dependent on deacetylation levels. In addition, water molecules also play an important role in the packing, conformation, and mechanical properties of chitin and chitosan-based materials.[36,37] In hydrated forms of chitosan, the packing structure can be stabilized by several hydrogen bonds mediated by water molecules without direct interactions between sheets.[23] However, the solution conformation and the influence of the solvent on these polymers remain unclear and under debate.[36,38,39]

Toward a better understanding of these interactions at a molecular level, we have performed molecular dynamics simulations of chitin and chitosan chains under different conditions to address the role of solvation in the hydrogen bond pattern, structure, and solubility of these polymers. Within this context, the influence of ionic strength on the conformation of chitin and the influence of pH in the conformation of chitosan are also discussed.

Methodology

Molecular Systems and Simulation. A modeled 10-mer polysaccharide filament with $\phi \sim -60°$ and $\varphi \sim +110°$ (where ϕ and φ are defined by atoms O5−C1−O1−C4 and C1−O1−C4−C3, respectively) was used as starting structural framework in all simulations. The systems are summarized in Table 1. The polymer chains were placed in a rectangular simulation box with dimensions of $x = 3.0$, $y = 3.0$, and $z = 5.0$ nm, where a covalent glycosidic bond, with the necessary bonded terms, was defined across the periodic box, hence treating the filaments as infinite chains. The nanoparticle was formed by 9 chitin filaments arranged in a 3×3 matrix in a β-chitin configuration. The systems were then solvated by filling the box with SPC water model molecules.[40] Sodium and chloride ions were used to achieve

Table 1. Description of the Simulated Systems

system[a]	no. of solute atoms	no. of ions	no. of solvent atoms	degree of acetylation (%)	ionic strength (mol.Kg^{-1})	pH[b]
CHT	170	0	1365	100	0.0	n/a
$CHT_{0.4}$	170	10	1355	100	0.4	n/a
$CHT_{1.1}$	170	30	1335	100	1.1	n/a
CHS_{LOW}	160	10	1473	0	0.4	low
$CHS_{NEUTRAL}$	155	10	1394	0	0.4	neutral
CHS_{HIGH}	150	10	1477	0	0.4	high
nanochitin[c]	1530	0	6310	100	0.0	n/a

[a] CHT: chitin; CHS: chitosan. [b] pH values corresponds to low <4; neutral = 6.5; high >10. [c] Corresponds to a 9-chain β-chitin nanoparticle arranged into a 3 × 3 matrix comprising a total of 90 N-acetyl-glucosamine residues.

the desired ionic strengths. Each system was energy minimized using 10,000 steps of the steepest descent method. After minimization the solvent was equilibrated by performing 10 ps molecular dynamics simulation at 50, 150, and 300K, with non-hydrogen atoms positionally restrained (force constant 1.0×10^3 kJ.mol^{-1}.nm^{-2}). Following the 30 ps solvent equilibration, a total of 30 ns for the chains and 20 ns for the nanoparticles molecular dynamics simulations were performed in an isothermal−isobaric (NPT) ensemble using the leapfrog algorithm[41] with a 1-fs time step, therefore allowing structural flexibility of the filament along its axis. The configurations were recorded every 1 ps for analysis. During the MD simulation, at every time step, the translational and rotational motion of the center of mass was removed. The temperature was kept at 300 K by coupling the solutes and the solvent separately to Berendsen thermostats[42] with a relaxation time of 0.1 ps. The pressure was maintained at 1 bar by coupling to a Berendsen barostat[42] via semi-isotropic coordinate scaling with a relaxation time of 10 ps and a compressibility of 4.5×10^{-6} (kJ.mol^{-1}.nm^{-3})$^{-1}$. Water stretching and bending motions were constrained using the LINCS algorithm.[43] A 1.4 nm cutoff was used for the short-range electrostatics and van der Waals interactions. Long-range electrostatic contributions were treated via the generalized reaction field[44] with ε=66. All simulations were carried out using extensions of the GROMOS carbohydrate force field[45] within the GROMACS 3.3.2 program.[46]

Electrostatic Potential and Solvation Free Energy Calculations. Electrostatic potential and solvation free energy calculations were obtained by solving numerically the nonlinear Poisson−Boltzmann equation and applying a finite-difference procedure,[47−49] which was performed using the APBS (Adaptive Poisson−Boltzmann Solver) program[50] in conjunction with the GROMOS point charge parameter set for carbohydrates.[45] A dielectric constant for solvent of 78.54 C^2/N.m^2 with solvent radius of 1.4 nm, surface tension of 0.105 N/m, and ionic strength of 0.4 mM was used to describe the structures in aqueous solution. The internal dielectric constant of the solute was set to 1 C^2/N.m^2, and the apolar contribution to the solvation free energy was calculated using gamma equal to 0.105 kJ/mol. The three-dimensional potentials were obtained using 129 grid points in the x, y, and z directions.

Results and Discussion

Ionic strength is well-known to play an important role on the ability of chitin and chitosan to aggregate forming different gels, beads, and nanoparticles in solution.[51] For example, a decrease of the persistence length of chitosan in gels has been proposed to be correlated with the increase of the ionic strength in the media.[51] Nevertheless, its effect on the chains of these polysaccharides remains elusive. Due to the nature of our setup, we are able to isolate the influence of the ionic strength on single chains of chitin in aqueous solution. It is worth noting that values of ϕ −60° and φ +110° were used as the starting point for all the initial structures. A time evolution analysis of chitin's ϕ and φ torsional angles shows the influence of the ionic strength on the structural convergence of the chitin chain, from the initial conformation (Figure 1a,b). It is clear from Figure 1 that an increase in ionic strength results in a slower convergence to its equilibrium structure. Chitin in the absence of salt reached its equilibrium structure (i.e., a 2-fold helix) after ca. 5 ns. To achieve this same configuration, a total of 25 ns of sampling were needed for the system with an ionic strength of 1.1 M NaCl. In all simulations the final values for ϕ and φ dihedral angles of fully solvated chains converge to the similar values of crystalline chitin. This is illustrated by the ϕ/φ maps for the last sampled 5 ns (Figure 1c-e). Available experimental values obtained by X-ray diffraction for two independent measurements for β-chitin and one for α-chitin crystal packing are also plotted for reference (Figure 1c-e). This result shows that fully solvated chitin chains tend to assume a typical nanoparticle crystal-like configuration and indicates that ionic strengths up to 1.1 M NaCl do not alter the equilibrium conformation of chitin in water at room temperature.

In order to further characterize the structure of chitin chains in aqueous solution, we have calculated its helicity as a function of the simulation time. It is well-known that the crystalline structure of chitin displays less conformational variability than chitosan.[13,23] The former maintains its configuration in the 2-fold helix and ϕ and φ values around −90° and +90°, respectively. On the other hand, chitosan can assume four main helical conformations: extended 2-fold helix, relaxed 2-fold helix, 4/1 helix, and 5/3 helix. The ϕ and φ values for chitosan in a 2-fold helix shifts slightly to $\phi \cong -98$ and $\varphi \cong 92$;[21] the 4/1 helix can exist in two forms, $\phi_1 = -66.4$, $\omega_1 = 121.6$ and $\phi_2 = -75.0$, $\omega_2 = 126.9$[28] and has a repetition unit composed of two residues, thus generating the full 4-fold helix using the space group $P4_1$ (2 residues with a translation after a 90° of rotation). No specific values of ϕ and φ are associated with 5-fold and relaxed 2-fold helices since they can adopt a wide range of values.[30,31] Due to the effects of solvation and higher temperature (300 K) on the polymer, compared to a crystal structure, we have chosen not to take into account the all crystalline parameters that define chitin and chitosan helical motifs.[23] Instead, the helical periodicity (helicity and chain repeat) was used as criterion, with a ±15°-variation allow-

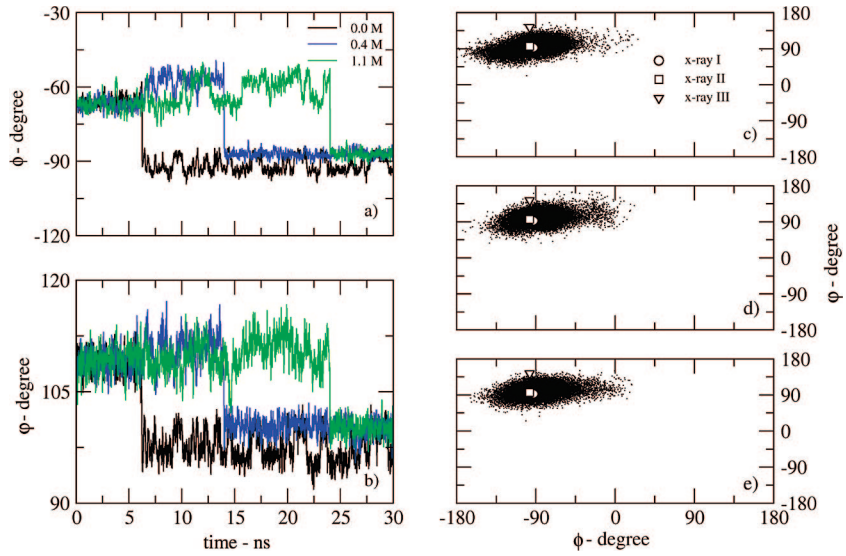

Figure 1. ϕ and φ torsional angles for chitin at different ionic strengths: a) and b) as a function of simulation time and c-e) distribution map for the last 5 ns for the systems at c) 0.0 M, d) 0.4 M, and e) 1.1 M ionic strength. Three independent experimentally determined values of ϕ and φ from α- (X-ray II[27]) and β-chitin (X-ray I;[34] X-ray III[26]) crystals are plotted for reference in c-e). a) and b) values are shown as a 20-ps interval averages.

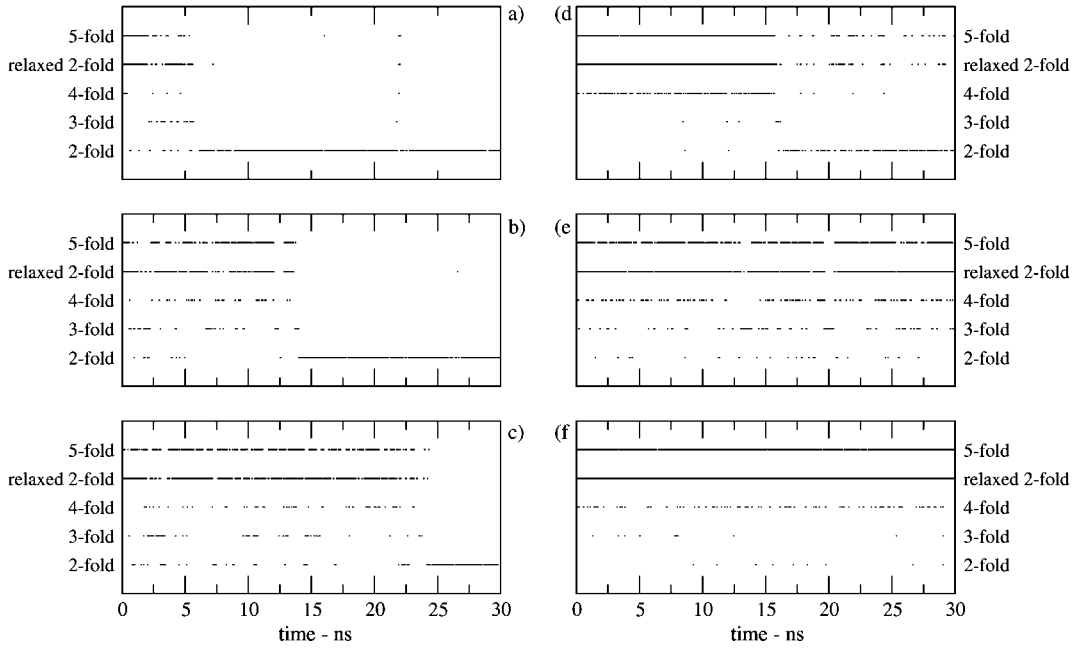

Figure 2. Structural pattern for a-c) chitin and d-f) chitosan chains in aqueous solution as a function of time: a) chitin, 0.0 M; b) chitin, 0.4 M; c) chitin 1.1 M; d) chitosan at high pH; e) chitosan at neutral pH; and f) chitosan at low pH.

ance. The algorithm employed here was based on the virtual bond method developed by Zugenmaier and Sarko to analyze the structure of fibrous polymers such as polysaccharides.[52] Thanks to the nature of our setup (i.e., an infinite chain along the periodic box) chitosan conformation was described according to Ogawa's classification of the crystal structure of chitosans.[23,53−55] According to this approach, five motifs have been probed: 2-fold helix (2 residues per turn forming a *zigzag* motif), 3-fold helix (right-handed helix with 3 residues per turn), 4-fold helix (right-handed helix with 8 residues per turn where four sets of two residues are rotated by 90° around the principal axis to complete one turn), relaxed 2-fold (right-handed helix with 8 residues per turn where two sets of four residues are rotated by 180° around the principal axis to complete one turn), and 5-fold helix (left-handed helix with 5 residues per turn). If the configuration of the entire chain, at any given time, fails to fulfill the requirements of each motif, it is then classified as having a random configuration, and it is not displayed in the presented graphs. (A graphical representation of the X-ray structures for the chitin and chitosan helical motifs can be found in a comprehensive review by Ogawa and coworkers).[23]

Time dependent evolution of helical configuration preferences are shown in Figure 2 for the chains at 0.0, 0.4, and 1.1 M ionic strength. Once again the structural behavior of the chains shows that chitin dynamics is slowed down with the increase of ionic strength, which seems to stabilize the

initial configuration (Figure 2). As expected, all the chains converge to the 2-fold helix, and no significant difference is observed in helical motif distributions for the last 5 ns of simulation. It is worth noting that all chains have visited all possible configurations before reaching equilibrium indicating that simulation setup is insensitive to the initial conformation (with the exception of the 2-fold helix motif). These findings indicate that chitin dynamics and conformation may be transiently altered by interactions with ionic species. This is supported by a recent experimental work where a solution of NaOH/urea (8 wt%/4 wt%, respectively) was shown to solubilize chitin at temperatures around −10 °C.[56] In the proposed mechanism, Na^+ ions would facilitate water molecules to enter and disrupt the crystalline structure of chitin by breaking interchain hydrogen bonds. The presence of urea was verified to be necessary to stabilize solubility as gelation would take place in the presence of the salt only. In the currently presented simulations, the highest ionic strength setup is equivalent to a solution of roughly 4 wt% NaCl concentration.

It is well-known that interchain hydrogen bonds in chitin are responsible for its highly stable crystalline state.[19,25,57] It is also known that N-acetylglucosamine is soluble in water and slightly soluble in ethanol. However, our results show that a chitin chain in aqueous solution shows low conformational exchange and similar degree of rigidity to the crystalline state (based on ϕ/φ distributions and helical conformation). This cannot be explained solely by the high torsional barrier around the glycosidic bond resulting from the anomeric effect, otherwise chitosan should also behave similarly, which is clearly not the case. Figure 2d-f shows that chitosan presents a higher conformational diversity than chitin, and it becomes less structured in acidic medium. At high pH, the 2-fold helix is clearly the dominant configuration followed by the 5-fold and relaxed 2-fold conformations. The 2-fold helix is rarely visited at neutral pH, and the less structured 5-fold and relaxed 2-fold are the two preferred conformations at low pH.

Analyses of the intrachain hydrogen bond pattern in chitin reveal only one persistent hydrogen bond, namely $HO3_{(n)}\cdots O5_{(n+1)}$, which seems to be the driving force behind the stabilization of chitin in a 2-fold helix motif (details in Figure 3). This interaction favors φ to adopt values locking the chain into the 2-fold configuration. A similar behavior was observed for the simulation of a β-chitin nanoparticle (Table 2). The β-nanochitin setup comprised 9 chains assembled in a 3 × 3 arrangement solvated by water molecules. Therefore the central chain in the system is completely shielded from water molecules. Analysis of the interactions of the central chain with the other filaments showed three types of persistent hydrogen bond. The intramolecular hydrogen bond $HO3_{(n)}\cdots O5_{(n+1)}$ and intermolecular hydrogen bonds between the N-acetyl groups of different chains have been both described to occur in crystals and are responsible for the bonded piles or sheet arrangement in chitin.[19,26] In addition to these interactions, our simulation shows that ca. 20% of the intermolecular hydrogen bonds are between the hydroxymethyl group of one chain with the N-acetyl group of another chain of the nanoparticle (Table 2). To date, these interactions have not been observed in crystals of β-chitin. This discrepancy may be due to i) the relatively low occurrence (20%) and weak character of these hydrogen bonds (lifetime is half of that of hydrogen bonds between two N-acetyl groups); ii) experimental measurements were obtained from anhydrous crystals, which typically display very low or no conformational variability; or iii) a combination of both. For the internal chain of the nanoparticle, the frequency of $O3\text{-}HO3_{(n)}\cdots O5_{(n+1)}$ intramolecular hydrogen bond reaches nearly 90%, and its lifetime increases almost 60% compared to the solvated chain. If the $O3\text{-}HO3_{(n)}\cdots O5_{(n+1)}$ intramolecular hydrogen bond is responsible for maintaining a chitin chain in a 2-fold helix motif and absence of solvation in these regions strengthens such interactions, it is reasonable to propose that solubility of chitin is inversely related to the stability of this interaction.

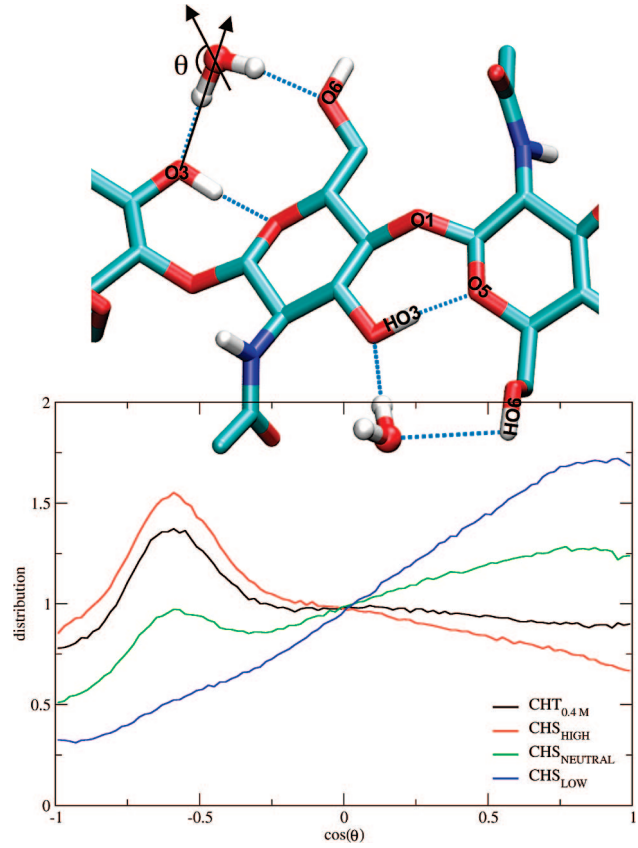

Figure 3. Solvent (water) orientation around the O3 oxygen atom of chitin and chitosan chains. Property is shown as the average orientation (cos θ) over the entire simulation for a 5-Å radius around the O3 atom. θ is defined by the angle formed between the vector formed by O3 and the water oxygen atoms and the water dipole vector (as illustrated by the black arrows). Hydrogen bonds are represented by dashed blue lines. Water molecules are displayed in a ball-and-stick model and the sugar units of chitin in sticks (atoms are color coded as cyan: carbon; blue: nitrogen, red: oxygen, and white: hydrogen).

In order to verify this hypothesis, three 30 ns simulations of fully solvated chitosan chains (100% N-deacetylated chitin) in water were carried out at low, ca. neutral, and high pH. It is worth noting that chitosan is only fully soluble at pH below 6.[13] The helical propensities and hydrogen-bond patterns were calculated for the three simulations and are

Table 2. Number and Lifetime of Hydrogen Bonds in Chitin and Chitosan Averaged for the Entire Trajectory

	$HO3_{(n)}\cdots O5_{(n+1)}$		$O3\text{-}HO3\cdots O_{WATER}$		$H_{WATER}\cdots O3$	
system	time[a]	number[b]	time[a]	number[b]	time[a]	number[b]
			Chitin			
CHT	6.13	0.69 ± 0.14	2.73	0.19 ± 0.11	3.10	1.08 ± 0.16
$CHT_{0.4}$	5.88	0.63 ± 0.15	3.32	0.24 ± 0.12	3.08	1.08 ± 0.16
$CHT_{1.1}$	5.34	0.58 ± 0.15	3.25	0.25 ± 0.13	3.02	1.08 ± 0.17
			Chitosan			
CHS_{LOW}	2.71	0.53 ± 0.14	1.69	0.27 ± 0.13	1.10	0.26 ± 0.14
$CHS_{NEUTRAL}$	4.83	0.48 ± 0.12	2.23	0.29 ± 0.13	2.26	0.72 ± 0.16
CHS_{HIGH}	5.60	0.59 ± 0.15	1.84	0.19 ± 0.12	2.66	1.25 ± 0.18

	$HO3_{(n)}\cdots O5_{(n+1)}$		NAc···NAc		$NAc\cdots OH_{MET}/OH_{MET}\cdots NAc$	
nanochitin (central chain)	time[a]	number[b]	time[a]	number[b]	time[a]	number[b]
			Chitin Nanoparticle			
	9.77	0.86 ± 0.11	7.61	0.51 ± 0.09	4.23	0.22 ± 0.14

[a] Time given in ps. [b] Average number per sugar unit; NAc: N-acetyl group; OH_{MET}: carbohydrate hydroxymethyl group.

illustrated in Figure 2d-f and Table 2. The average number of the $HO3_{(n)}\cdots O5_{(n+1)}$ intrachain hydrogen bond in chitosan is not significantly different from the observed values in chitin or as a function of the pH. However, dramatic changes are observed in i) the number of water molecules hydrogen bonding O3 and ii) the lifetime of the $HO3_{(n)}\cdots O5_{(n+1)}$ interaction. The higher the pH the closer these numbers are to the values observed in chitin. For example, for chitosan in low pH the $HO3_{(n)}\cdots O5_{(n+1)}$ hydrogen bond lifetime is only half of the value of chitin (3 versus 6 ps, respectively), while for chitosan at high pH the values for the average number and residence time of a water molecule interacting with O3 is nearly identical to the values observed in chitin. These differences in residence times suggest that chain conformation and solubility are affected by microsolvation entropy.

To probe such a hypothesis, the orientation of all the water molecules within a 5-Å radius from all O3 atoms was calculated and averaged over the entire simulation. It is displayed in Figure 3 as the cosine of the angle (θ) formed by the dipole vector of the water molecule with the vector defined by O3 with the water oxygen. The averaged water molecule orientation profile for chitin at 0.4 M is shown along with the profiles for chitosan chains at the same ionic strength but at different pH values. No significant difference was observed for the solvent orientation profile of chitin as a function of ionic strength (data not shown for conciseness). The peak observed for chitin around −0.7 is due to a hydrogen atom of a water molecule that interacts with the oxygen atom O3 of the sugar ring, leaving the HO3 available to hydrogen bond the O5 oxygen atom of the next sugar unit. The spatial distribution of the N-acetyl and the hydroxylmethyl groups define a pocket, which is occupied by a water molecule. The position of this water molecule is stabilized by a hydrogen bond with either the hydrogen or oxygen atom of the hydroxymethyl group of the neighboring sugar (Figure 3). The NAc groups were not observed to take part in this arrangement.

Accordingly for chitosan, the solvent orientation profile around the region becomes increasingly similar to chitin's profile as pH increases, which leads to a decrease in solubility. A nearly identical profile for the orientation and distribution of the water molecules around this region is observed for chitin and chitosan at high pH (the two most insoluble species). The analysis of the electrostatic potential reveals an increased availability of negatively charged sites at the surface of chitosan with the increase of pH (Figure 4). It does not come as a surprise the fact that the molecular surfaces of chitin and chitosan at high pH exhibit a similar electrostatic profile (Figure 4). The visualization of this property allows the understanding of how water molecules are solvating the polymer. The waters in the first solvation shell of chitosan at low pH interact with the sugars mainly via their oxygen atoms. In contrast, a considerably large amount of water molecules would hydrogen bond chitin via their hydrogen atoms (as is shown in Figure 3). The conformational variation of the chitosan chains is also in

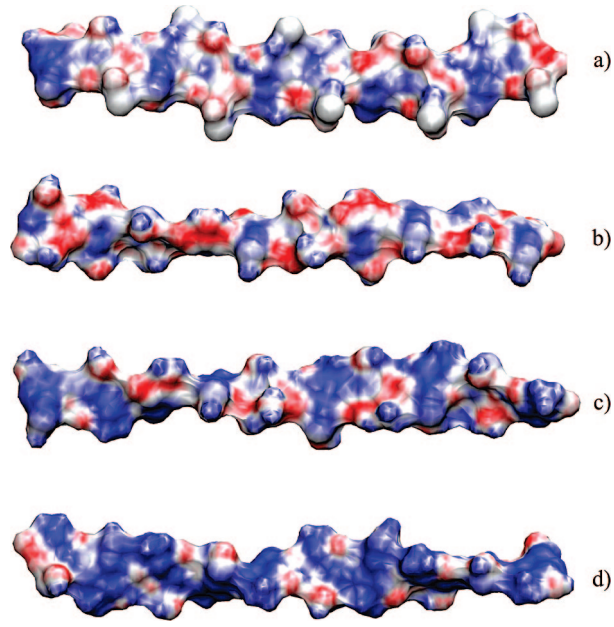

Figure 4. Electrostatic potential plotted onto the molecular surface of a) chitin and b-d) chitosan; b) chitosan at high pH; c) chitosan at neutral pH; and d) chitosan at low pH. Positive (blue) and negative (red) potentials correspond to the range of $-50\ k_BT/e$ to $+\ 50\ k_BT/e$.

Table 3. Residue Average Contribution (kcal/mol) to the Free Energy of Solvation of Chitin and Chitosan Chains

system	$\Delta G_{ELECTROSTATIC}$	ΔG_{APOLAR}	ΔG
$CHT_{0.4}$	−15.0	6.1	−8.9
CHS_{LOW}	−50.6	5.2	−45.4
$CHS_{NEUTRAL}$	−27.4	5.2	−22.2
CHS_{HIGH}	−15.2	5.3	−9.9

accordance with the hypothesis that the stability of the intramolecular $HO3_{(n)}\cdots O5_{(n+1)}$ hydrogen bond favors the 2-fold helical configuration. Time dependent conformational analysis of the chitosan simulations show that the 2-fold helix motif is rarely visited by the chain at low pH (soluble). This trend is altered by pH increase, and the 2-fold helix motif becomes the most representative configuration for the setup at high pH (Figure 2d-f).

A number of contributing components to chitosan solubility, such as intramolecular hydrogen bonding, van der Waals forces, and hydrophobic interactions, have been reported.[58−60] However, a recent experimental study suggests that the solubility of chitosan in aqueous solution is primarily attributed to electrostatics forces between the polymer and the medium.[61] To shed some light on the problem, the electrostatics and apolar contributions to the free energy of solvation of chitin and chitosan chains were calculated via Poisson−Boltzmann electrostatics using the APBS program[50] (see Methodology). Representative structures having their corresponding equilibrium conformation were selected from the last 5 ns of each simulation with the same ionic strength, so that pH was the only variable among the different chitosan chains. The contributions to the free energy of solvation were calculated and are presented in Table 3 as the average contribution per residue.

The estimated solvation free energy values cannot be compared to experimental values due to the absence of such measurements in the literature. However, in agreement with experimental observations on chitin and chitosan solubility, a clear trend shows that chitosan at low pH is the most soluble form, whereas chitin and chitosan at basic pH are the least soluble chains. This suggests that these calculations can be potentially used to predict relative solubility for the different forms of chitosan. Once again, remarkable similarities can be seen for the calculated solvation free energy contributions for chitin and chitosan chains at basic pH. It is also clear that solubility in chitin and chitosan chains is mainly driven by electrostatic contributions. Moreover, it is interesting to note that the electrostatic contributions to the solvation free energy are inversely proportional to the residence times of the intramolecular $HO3_{(n)}\cdots O5_{(n+1)}$ hydrogen bond and highly correlated with the average orientation of water molecules around the O3 oxygen. We have also investigated the influence of different ionic strengths on the electrostatic contribution. The latter is restricted to a few percentile units for salt concentrations from 0.15 to 1.10 mM (data not shown for conciseness).

Conclusion

We have shown from a series of molecular dynamics simulations of chitin and chitosan chains that the flexibility of the polysaccharide chain is inversely related to the stability of the intramolecular hydrogen bond between the atom HO3 of one sugar unit and the O5 atom of the next monosaccharide. As experimentally observed for crystals, solvated chitin chains also assume mostly the 2-fold helix motif, and its equilibrium conformation was not affected by ionic strengths up to 1.1 M, in agreement with rheological studies of chitin in solution that portrays it as a semirigid polysaccharide.[13] The stability of the intrachain hydrogen bond $HO3_{(n)}\cdots O5_{(n+1)}$ seems to be heavily affected by water exchange and residency times in its neighborhood. It presents a higher persistence in the internal chains of nanoparticles where the presence of the solvent is excluded. Although weak and of low occurrence, our simulation suggests that intermolecular hydrogen bonds between the hydroxymethyl and N-acetyl groups are also present in solvated β-chitin nanoparticles. The charged amino group (NH_3^+) at the neighboring C2 atom of chitosan at low pH values seems to increase water exchange in the region of the O3 atom destabilizing the $HO3_{(n)}\cdots O5_{(n+1)}$ hydrogen bond. This interaction in chitin and chitosan is responsible for locking the polymer conformation into a 2-fold helical motif, reducing conformational variability. The calculated solvation free energies indicate that solubility in chitosan is controlled mainly by electrostatic interactions. The high correlation of the electrostatic contributions to the solvation free energies with hydrogen bond patterns suggest that the solubility of these polymers is inversely related to their ability to form intramolecular $HO3_{(n)}\cdots O5_{(n+1)}$ hydrogen bonds. The presented data draw for the first time a parallel between the intrachain hydrogen bond pattern in chitin and chitosan chains and their solubility. These findings are expected to provide insights into the rationale of chitin and chitosan-based nanomaterial design.

Acknowledgment. E.F.F. and L.C.G.F. acknowledge CAPES, CNPq, and FAPESP for financial support. The authors thank Peter Zugenmaier for providing the formalism for structural characterization of crystalline chitins and Nathan Baker for help with the APBS program. Gratitude is expressed to Brian Lower for careful reading of this manuscript and to the Environmental Molecular Sciences Laboratory through the Computational Grand Challenge Application GC20892. This work has been partly supported by the DOE Office of Advanced Scientific Computing Research through the project "Data Intensive Computing for Complex Biological Systems". Pacific Northwest National Laboratory is operated for the DOE by Battelle Memorial Institute under contract DE-AC05-76RLO1830.

References

(1) Sannan, T.; Kurita, K.; Iwakura, Y. Studies on Chitin. 2. Effect of Deacetylation on Solubility. *Makomol. Chem.* **1976**, *177* (12), 3589–3600.

(2) Gibbs, G.; Tobin, J. M.; Guibal, E. Sorption of Acid Green 25 on Chitosan: Influence of Experimental Parameters on Uptake Kinetics and Sorption Isotherms. *J. Appl. Polym. Sci.* **2003**, *90* (4), 1073–1080.

(3) Knorr, D. Dye Binding-Properties of Chitin and Chitosan. *J. Food Sci.* **1983**, *48* (1), 36–37.

(4) Maghami, G. G.; Roberts, G. A. F. Studies on the Adsorption of Anionic Dyes on Chitosan. *Makromol. Chem.* **1988**, *189* (10), 2239–2243.

(5) Uragami, T.; Yoshida, F.; Sugihara, M. Studies of Synthesis and Permeabilities of Special Polymer Membranes 0.51. Active-Transport of Halogen Ions through Chitosan Membranes. *J. Appl. Polym. Sci.* **1983**, *28* (4), 1361–1370.

(6) Liu, C. X.; Bai, R. B. Adsorptive Removal of Copper Ions with Highly Porous Chitosan/Cellulose Acetate Blend Hollow Fiber Membranes. *J. Membr. Sci.* **2006**, *284* (1−2), 313–322.

(7) Vieira, R. S.; Beppu, M. M. Dynamic and Static Adsorption and Desorption of Hg(II) Ions on Chitosan Membranes and Spheres. *Water Res.* **2006**, *40* (8), 1726–1734.

(8) Zhou, D.; Zhang, L.; Guo, S. L. Mechanisms of Lead Biosorption on Cellulose/Chitin Beads. *Water Res.* **2005**, *39* (16), 3755–3762.

(9) Dutta, P. K.; Dutta, J.; Tripathi, V. S. Chitin and Chitosan: Chemistry, Properties and Applications. *J. Sci. Ind. Res.* **2004**, *63* (1), 20–31.

(10) Kim, I. Y.; Seo, S. J.; Moon, H. S.; Yoo, M. K.; Park, I. Y.; Kim, B. C.; Cho, C. S. Chitosan and Its Derivatives for Tissue Engineering Applications. *Biotechnol. Adv.* **2008**, *26* (1), 1–21.

(11) Ravi Kumar, M. N. V. A Review of Chitin and Chitosan Applications. *React. Funct. Polym.* **2000**, *46* (1), 1–27.

(12) Revoredo, O. B.; Nieto, O. M.; Suarez, Y.; Garcia, V.; Fernandez, M.; Iraizoz, A.; Henriques, R. D. Applications of Chitin and Chitosan in Pharmacy and Cosmetology. *Eur. J. Pharm. Sci.* **2006**, *28*, S7–S8.

(13) Rinaudo, M. Chitin and Chitosan: Properties and Applications. *Prog. Polym. Sci.* **2006**, *31* (7), 603–632.

(14) Ruel-Gariepy, E.; Leroux, J. C. *Chitosan: A Natural Polycation with Multiple Applications*; American Chemical Society: Montreal, 2006; p 384.

(15) Smitha, B.; Sridhar, S.; Khan, A. A. Chitosan-Poly(Vinyl Pyrrolidone) Blends as Membranes for Direct Methanol Fuel Cell Applications. *J. Power Sources* **2006**, *159* (2), 846–854.

(16) Rudall, K. M.; Kenching, W. Chitin System. *Biol. Rev. Camb. Philos. Soc.* **1973**, *48* (4), 597.

(17) Sugiyama, J.; Boisset, C.; Hashimoto, M.; Watanabe, T. Molecular Directionality of Beta-Chitin Biosynthesis. *J. Mol. Biol.* **1999**, *286* (1), 247–255.

(18) Atkins, E. Conformations in Polysaccharides and Complex Carbohydrates. *J. Biosci. (Bangalore)* **1985**, *8* (1−2), 375–387.

(19) Jang, M. K.; Kong, B. G.; Jeong, Y. I.; Lee, C. H.; Nah, J. W. Physicochemical Characterization of Alpha-Chitin, Beta-Chitin, and Gamma-Chitin Separated from Natural Resources. *J. Polym. Sci., Part A: Polym. Chem.* **2004**, *42* (14), 3423–3432.

(20) Kameda, T.; Miyazawa, M.; Ono, H.; Yoshida, M. Hydrogen Bonding Structure and Stability of Alpha-Chitin Studied by C-13 Solid-State Nmr. *Macromol. Biosci.* **2005**, *5* (2), 103–106.

(21) Yui, T.; Imada, K.; Okuyama, K.; Obata, Y.; Suzuki, K.; Ogawa, K. Molecular and Crystal-Structure of the Anhydrous Form of Chitosan. *Macromolecules* **1994**, *27* (26), 7601–7605.

(22) Okuyama, K.; Noguchi, K.; Miyazawa, T.; Yui, T.; Ogawa, K. Molecular and Crystal Structure of Hydrated Chitosan. *Macromolecules* **1997**, *30* (19), 5849–5855.

(23) Ogawa, K.; Yui, T.; Okuyama, K. Three D Structures of Chitosan. *Int. J. Biol. Macromol.* **2004**, *34* (1−2), 1–8.

(24) Mogilevskaya, E. L.; Akopova, T. A.; Zelenetskii, A. N.; Ozerin, A. N. The Crystal Structure of Chitin and Chitosan. *Polym. Sci., Ser. A* **2006**, *48* (2), 116–123.

(25) Blackwel, J. Structure of Beta-Chitin or Parallel Chain Systems of Poly-Beta-(1•4)-N-Acetyl-D-Glucosamine. *Biopolymers* **1969**, *7* (3), 281–298.

(26) Gardner, K. H.; Blackwell, J. Refinement of Structure of Beta-Chitin. *Biopolymers* **1975**, *14* (8), 1581–1595.

(27) Minke, R.; Blackwell, J. Structure of Alpha-Chitin. *J. Mol. Biol.* **1978**, *120* (2), 167–181.

(28) Lertworasirikul, A.; Yokoyama, S.; Noguchi, K.; Ogawa, K.; Okuyama, K. Molecular and Crystal Structures of Chitosan/Hi Type I Salt Determined by X-Ray Fiber Diffraction. *Carbohydr. Res.* **2004**, *339* (4), 825–833.

(29) Okuyama, K.; Noguchi, K.; Kanenari, M.; Egawa, T.; Osawa, K.; Ogawa, K. Structural Diversity of Chitosan and Its Complexes. *Carbohydr. Polym.* **2000**, *41* (3), 237–247.

(30) Lertworasirikul, A.; Tsue, S.; Noguchi, K.; Okuyama, K.; Ogawa, K. Two Different Molecular Conformations Found in Chitosan Type II Salts. *Carbohydr. Res.* **2003**, *338* (11), 1229–1233.

(31) Kawahara, M.; Yui, T.; Oka, K.; Zugenmaier, P.; Suzuki, S.; Kitamura, S.; Okuyama, K.; Ogawa, K. Fourth 3d Structure of the Chitosan Molecule: Conformation of Chitosan in Its Salts with Medical Organic Acids Having a Phenyl Group. *Biosci. Biotechnol. Biochem.* **2003**, *67* (7), 1545–1550.

(32) Carlstrom, D. The Crystal Structure of Alpha-Chitin (Poly-N-Acetyl-D-Glucosamine). *J. Biophys. Biochem. Cytol.* **1957**, *3* (5), 669–683.

(33) Ramarkrishnan, C.; Prasad, N. Study of Hydrogen Bonds in Amino Acids and Peptides. *Int. J. Protein Res.* **1971**, *3* (4), 209–231.

(34) Yui, T.; Taki, N.; Sugiyama, J.; Hayashi, S. Exhaustive Crystal Structure Search and Crystal Modeling of Beta-Chitin. *Int. J. Biol. Macromol.* **2007**, *40* (4), 336–344.

(35) Dweltz, N. E. Structure of Beta-Chitin. *Biochim. Biophys. Acta* **1961**, *51* (2), 283–294.

(36) Li, Q. X.; Song, B. Z.; Yang, Z. Q.; Fan, H. L. Electrolytic Conductivity Behaviors and Solution Conformations of Chitosan in Different Acid Solutions. *Carbohydr. Polym.* **2006**, *63* (2), 272–282.

(37) Mazeau, K.; Rinaudo, M. The Prediction of the Characteristics of Some Polysaccharides from Molecular Modeling. Comparison with Effective Behavior. *Food Hydrocolloids* **2004**, *18* (6), 885–898.

(38) Pedroni, V. I.; Gschaider, M. E.; Schulz, P. C. Uv Spectrophotometry: Improvements in the Study of the Degree of Acetylation of Chitosan. *Macromol. Biosci.* **2003**, *3* (10), 531–534.

(39) Pedroni, V. I.; Schulz, P. C.; Gschaider, M. E.; Andreucetti, N. Chitosan Structure in Aqueous Solution. *Colloid Polym. Sci.* **2003**, *282* (1), 100–102.

(40) Berendsen, H. J. C.; Grigera, J. R.; Straatsma, T. P. The Missing Term in Effective Pair Potentials. *J. Phys. Chem.* **1987**, *91* (24), 6269–6271.

(41) Hockney, R. W. The Potential Calculation and Some Applications. In *Methods in Computational Physics*; Alder, B., Fernbach, S., Rotenberg, M., Eds.; Academic Press: New York/London, 1970; Vol. 9.

(42) Berendsen, H. J. C.; Postma, J. P. M.; Van Gunsteren, W. F.; Dinola, A.; Haak, J. R. Molecular-Dynamics with Coupling to an External Bath. *J. Chem. Phys.* **1984**, *81* (8), 3684–3690.

(43) Hess, B.; Bekker, H.; Berendsen, H. J. C.; Fraaije, J. Lincs: A Linear Constraint Solver for Molecular Simulations. *J. Comput. Chem.* **1997**, *18* (12), 1463–1472.

(44) Tironi, I. G.; Sperb, R.; Smith, P. E.; Van Gunsteren, W. F. A Generalized Reaction Field Method for Molecular-Dynamics Simulations. *J. Chem. Phys.* **1995**, *102* (13), 5451–5459.

(45) Lins, R. D.; Hunenberger, P. H. A New Gromos Force Field for Hexopyranose-Based Carbohydrates. *J. Comput. Chem.* **2005**, *26* (13), 1400–1412.

(46) Van der Spoel, D.; Lindahl, E.; Hess, B.; Groenhof, G.; Mark, A. E.; Berendsen, H. J. C. Gromacs: Fast, Flexible, and Free. *J. Comput. Chem.* **2005**, *26* (16), 1701–1718.

(47) Davis, M. E.; McCammon, J. A. Calculating Electrostatic Forces from Grid-Calculated Potentials. *J. Comput. Chem.* **1990**, *11* (3), 401–409.

(48) Antosiewicz, J.; Gilson, M. K.; McCammon, J. A. Acetylcholinesterase - Effects of Ionic-Strength and Dimerization on the Rate Constants. *Isr. J. Chem.* **1994**, *34* (2), 151–158.

(49) Nicholls, A.; Honig, B. A Rapid Finite-Difference Algorithm, Utilizing Successive over-Relaxation to Solve the Poisson-Boltzmann Equation. *J. Comput. Chem.* **1991**, *12* (4), 435–445.

(50) Holst, M.; Baker, N.; Wang, F. Adaptive Multilevel Finite Element Solution of the Poisson-Boltzmann Equation I. Algorithms and Examples (Vol 21, Pg 1319, 2000). *J. Comput. Chem.* **2001**, *22* (4), 475–475.

(51) Vachoud, L.; Zydowicz, N.; Domard, A. Physicochemical Behaviour of Chitin Gels. *Carbohydr. Res.* **2000**, *326* (4), 295–304.

(52) Zugenmaier, P.; Sarko, A. In *The Variable Virtual Bond, Fiber Diffraction Methods, 1980*; French, A. D., Gardner, K. H., Eds.; American Chemical Society: Washington, DC, ACS Symposium Series, 1980; pp 225−237.

(53) Ogawa, K. Chain Conformation of Chitin and Chitosan. *J. Agric. Chem. Soc. Japan* **1988**, *62* (8), 1225–1228.

(54) Ogawa, K.; Yui, T. Crystallinity of Partially N-Acetylated Chitosans. *Biosci. Biotechnol. Biochem.* **1993**, *57* (9), 1466–1469.

(55) Ogawa, K.; Yui, T. Effect of Explosion on the Crystalline Polymorphism of Chitin and Chitosan. *Biosci. Biotechnol. Biochem.* **1994**, *58* (5), 968–969.

(56) Hu, Y.; Ding, Y.; Ding, D.; Sun, M. J.; Zhang, L. Y.; Jiang, X. Q.; Yang, C. Z. Hollow Chitosan/Poly(Acrylic Acid) Nanospheres as Drug Carriers. *Biomacromolecules* **2007**, *8* (4), 1069–1076.

(57) Mazeau, K.; Winter, W. T.; Chanzy, H. Molecular and Crystal Structure of a High-Temperature Polymorph from Chitosan and Electron Diffraction Data. *Macromolecules* **1994**, *27*, 7606–7612.

(58) Amiji, M. M. Pyrene Fluorescence Study of Chitosan Self-Association in Aqueous Solution. *Carbohydr. Polym.* **1995**, *26*, 211–213.

(59) Nystrom, B.; Kjoniksen, A. L.; Iversen, C. Characterization of Association Phenomena in Aqueous Systems of Chitosan of Different Hydrophobicity. *Adv. Colloid Interface Sci.* **1999**, *79*, 81–103.

(60) Philippova, O. E.; Volkov, E. V.; Sitnikova, N. L.; Khokhlov, A. R.; Desbrieres, J.; Rinaudo, M. Two Types of Hydrophobic Aggregates in Aqueous Solutions of Chitosan and Its Hydrophobic Derivative. *Biomacromolecules* **2001**, *8* (2), 483–490.

(61) Lavertu, M.; Filion, D.; Buschmann, D. Heat-Transfer of Protons from Chitosan to Glycerol Phosphate Chitosan Precipitation and Gelation. *Biomacromolecules* **2008**, *9*, 640–650.

CT8002964